# Characterization of Fullerenes by Mass Spectrometry

STEPHEN W. MCELVANY, MARK M. ROSS,* and JOHN H. CALLAHAN

*Mass Spectrometry & Ion Chemistry Section, Chemistry Division/Code 6113, Naval Research Laboratory, Washington, D.C. 20375-5000*

*Received December 16, 1991 (Revised Manuscript Received January 15, 1992)*

## Introduction

Research on the recently-discovered new form of carbon, fullerenes, is expanding at a rapid rate. As explained elsewhere in this issue, this new scientific field has emerged from fundamental studies of gas-phase carbon clusters.[1] This research, largely based on mass spectrometry experiments,[2-5] provided the crucial evidence for postulation of the fullerene structures.[4] This led to further experimental and theoretical work and, finally, to the discovery of a method by which large quantities of fullerenes can be synthesized.[6] The purpose of this Account is to describe some of the key, early mass spectrometric studies of gas-phase carbon clusters, which served as a prelude to the Huffman–Krätschmer discovery, as well as some more recent investigations of fullerene properties in the gas phase.

Mass spectrometry has proven invaluable in the study of carbon cluster production mechanisms and properties, and more recently for characterization of fullerenes and fullerene derivatives, because it is a sensitive, specific, and versatile technique. The fundamentals of mass spectrometry are simple: neutral molecules are ionized and separated by their mass-to-charge ratio ($m/z$). A typical experiment begins with ionization of a volatile species, either by electron ionization (EI) or by protonation in a reagent gas plasma (chemical ionization, CI). Involatile species can be desorbed and ionized by various techniques including thermal desorption EI or CI, laser desorption/vaporization (LD/LV), and particle bombardment. Following ionization, two general approaches are used for ion mass analysis. With "beam" instruments, ions are accelerated out of the ion source and separated according to momentum (magnet, B), kinetic energy (electric sector, E), mass (quadrupole, Q) or flight time (time-of-flight, TOF). Alternatively, ions can be trapped and analyzed using a quadrupole ion storage device or a Fourier transform ion cyclotron resonance (ICR) mass spectrometer (FTMS). The resultant spectrum of the ion and its fragments can give both molecular weight and structural information.

The power of mass spectrometry is enhanced by the development of tandem mass spectrometry (MS/MS) techniques, which further extend the capability to probe ion structures and properties. In one type of MS/MS

experiment, known as collision-induced dissociation (CID), one mass analyzer is used to select an ion of a particular mass-to-charge ratio. The selected ion is then collided with a neutral target gas, after which the fragments from the collision are analyzed by a second mass analyzer. At low ion kinetic energies, reactions between the selected ion and reagent gases can be studied. The availability of numerous ionization and mass analysis methods has given rise to a variety of instruments that can be applied to a range of analytical problems. Much of the initial work on buckminsterfullerene and its derivatives has relied in part on analytical characterization by mass spectrometry.

## Early Studies of Carbon Clusters

The initial mass spectrometric studies by groups at Exxon,[2] Bell Labs,[3] and Rice[4,5] reported the production of large carbon clusters ($n > 30$) and showed certain anomalously abundant cluster sizes. The method used by the these groups to produce carbon clusters was developed by Smalley in the early 1980s[7] and consists of laser vaporization of a graphite rod, which is rotated and translated, followed by entrainment of the ablated species in a molecular beam. The nascent ions or photoionized neutrals were mass analyzed by TOFMS. Cluster research at the Naval Research Laboratory (NRL) at this time was focused on the production of clusters from a variety of materials using particle bombardment and laser vaporization in sector and TOF instruments.[8,9] While the cluster ion size distributions for most systems show a pseudoexponential decrease in abundance for larger species,[10] the bimodal distribution of positively-charged carbon cluster ions reported by the Exxon group[2] ($C_n^+$, $3 < n < 30$ with $\Delta n = 1$ and $n > 32$ with $\Delta n = 2$) was distinctive. This unique behavior and the unusual, anomalously abundant carbon cluster sizes ($C_n^+$, odd $n = 7, 11, 15, 19,$ and 23 in the low mass distribution and even $n = 50, 60,$ and 70 for the larger species) raised questions about the

Stephen W. McElvany received a B.S. degree from the College of Wooster and a Ph.D. degree from Michigan State University and, following a National Research Council Postdoctoral Associateship at the NRL, became a staff scientist in 1987.

Mark M. Ross received a B.A. degree from the University of Virginia and a Ph.D. degree from the Pennsylvania State University and, following a National Research Council Postdoctoral Associateship at the NRL, became a staff scientist in 1983.

John H. Callahan received a B.A. degree from the Colorado College and a Ph.D. degree from the University of Illinois and, following a National Research Council Postdoctoral Associateship at the NRL, became a staff scientist in 1987.

The authors' research interests include gas-phase ion chemistry, ion/surface interactions, analytical mass spectrometry, and of course, fullerenes.

(1) Smalley, R. E. *The Sciences* **1991,** *31,* 22. Kroto, H. W.; Allaf, A. W.; Balm, S. P. *Chem. Rev.* **1991,** *91,* 1213. Curl, R. F.; Smalley, R. E. *Sci. Am.* **1991,** *Oct,* 54.

(2) Rohlfing, E. A.; Cox, D. M.; Kaldor, A. *J. Chem. Phys.* **1984,** *81,* 3322.

(3) Bloomfield, L. A.; Geusic, M. E.; Freeman, R. R.; Brown, W. L. *Chem. Phys. Lett.* **1985,** *121,* 33.

(4) Kroto, H. W.; Heath, J. R.; O'Brien, S. C.; Curl, R. F.; Smalley, R. E. *Nature* **1985,** *318,* 162.

(5) Heath, J. R.; O'Brien, S. C.; Zhang, Q.; Liu, Y.; Curl, R. F.; Kroto, H. W.; Tittel, F. K.; Smalley, R. E. *J. Am. Chem. Soc.* **1985,** *107,* 7779.

(6) Krätschmer, W.; Lamb, L. D.; Fostiropoulos, K.; Huffman, D. R. *Nature* **1990,** *347,* 354.

(7) Dietz, T. G.; Duncan, M. A.; Powers, D. E.; Smalley, R. E. *J. Chem. Phys.* **1981,** *74,* 6511.

(8) Campana, J. E.; Barlak, T. M.; Colton, R. J.; DeCorpo, J. J.; Wyatt, J. R.; Dunlap, B. I. *Phys. Rev. Lett.* **1981,** *47,* 1046. Barlak, T. M.; Campana, J. E.; Colton, R. J.; DeCorpo, J. J.; Wyatt, J. R. *J. Phys. Chem.* **1981,** *85,* 3850.

(9) Colton, R. J.; Kidwell, D. A.; Ross, M. M. In *Mass Spectrometry in the Analysis of Large Molecules;* John Wiley & Sons: New York, NY, 1986; p 13. Freas, R. B.; Campana, J. E. *J. Am. Chem. Soc.* **1985,** *107,* 6202.
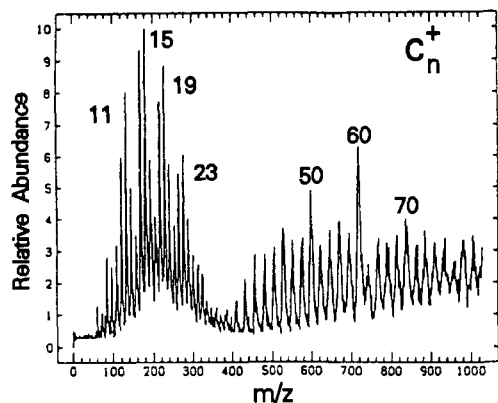
(10) Benninghoven, A.; Rudenauer, F. G.; Werner, H. W. *Secondary Ion Mass Spectrometry;* John Wiley & Sons: New York, NY, 1987; p 240.

**Figure 1.** Time-of-flight mass spectrum of nascent $C_n^+$ generated by direct laser vaporization (DLV) of a stationary graphite sample, showing the bimodal distribution and magic numbers at $n = 11$, 15, 19, 23, 50, 60, and 70.

mechanism of carbon cluster production and cluster properties.

Our initial experiments were directed at the mechanism(s) of carbon cluster formation and, in particular, why the low-mass $C_n^+$ distribution was observed by laser vaporization of graphite both with *and* without[11] a molecular beam, but the high-mass clusters were observed only with the molecular beam. In order to simplify the method, we designed our experiment to allow observation of the cluster ions formed directly in the plasma that is generated by laser irradiation of graphite, without subsequent collisions in a molecular beam or ionization. The ions produced by direct laser vaporization (DLV) (Nd:YAG, 532 nm) of a *stationary* graphite sample pellet were extracted at a right angle to the incident laser irradiation and mass analyzed by TOFMS. Initially, only the low-mass $C_n^+$ ($n < 30$) were observed, but after a few minutes of laser irradiation of the same spot on the target, the spectrum shown in Figure 1 was obtained.[12] This spectrum shows both low- and high-mass $C_n^+$, and the distribution is nearly identical to that measured originally by the Exxon group[2] using a molecular beam. This unexpected observation was postulated to result from the laser "drilling" a channel in the graphite pellet, which provided a confined space with higher particle densities where reactions could occur to yield the high-mass $C_n^+$. This was the first demonstration that large carbon clusters could be produced without a molecular beam, but the full significance was not realized at the time, i.e., the possibility of generating large quantities of these species from different carbonaceous materials and by a variety of techniques.

Another result from the TOFMS studies was that the larger $C_n^+$ were emerging from the laser-induced plasma with lower velocities than the smaller $C_n^+$. We speculated that this could in part explain why only the smaller $C_n^+$ were observed by DLV of graphite in an FTMS.[13] In this instrument the laser beam, and hence the plasma, propagates perpendicularly to the magnetic field and vaporizes a graphite sample located flush with

the ICR cell. The ions are constrained in cyclotron orbits around the magnetic field lines while the neutrals expand freely into the cell. This reduces ion/neutral interactions and preferentially samples those ions with velocities great enough to get into the center of the cell for trapping and analysis. However, in an FTMS equipped with a superconducting magnet, the laser vaporization occurs along the magnetic field lines, and as predicted, when DLV of graphite was studied in this experimental configuration, both low- and high-mass $C_n^+$ ($40 < n < 180$) species were observed.[14] In this case, the laser-induced plasma expands parallel to the magnetic field and both neutrals and ions propagate freely in a process similar to that in the field-free region between the sample and ion source in the TOFMS.

The first production of large $C_n^+$ in an FTMS allowed numerous studies of their properties[14] and prompted many other groups to use DLV of a variety of carbonaceous materials to generate carbon clusters.[15] The higher mass resolution afforded by FTMS (compared to TOFMS) was used to measure the isotopic ratios of $m/z$ 720 ($^{12}C_{60}^+$), $m/z$ 721 ($^{13}C^{12}C_{59}^+$), and $m/z$ 722 ($^{13}C_2^{12}C_{58}^+$), which showed that there is no detectable contribution from hydrogenated species in the high mass $C_n^+$ region.[14] In addition, the FTMS allowed the study of ion/molecule reactions and CID of $C_n^+$. While reactivity studies have shown the smaller $C_n^+$ to be reactive with several reagent gases,[16,17] which revealed isomeric structures and evidence for conversion from linear to cyclic structures between $n = 9$ and 10, the larger $C_n^+$ were found to be unreactive.[14] In addition, CID and IR photoactivation of the larger $C_n^+$ yielded no fragment ions, thus providing further evidence for unusual stability.

## Ion/Molecule Reactions of Fullerenes: Physical Properties

The early characterization of fullerene ions using the MS/MS capabilities afforded by FTMS was quite limited. Although the carbon cluster ions with $n > 10$ are relatively inert, electron-transfer (i.e., charge-transfer) reactions in the gas phase have been used successfully to bracket their ionization energies (IEs).[17-19] In brief, once the cluster ions are mass-selected (size-selected) and thermalized in the FTMS, reaction 1 is studied with neutrals (M) of differing IEs:

$$C_n^+ + M \rightarrow M^+ + C_n \qquad (1)$$
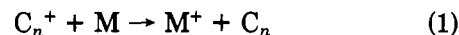
The IE of $C_n$ is then bracketed (relative to M) by determining if reaction 1 is exothermic (IE($C_n$) > IE(M)) or endothermic (IE($C_n$) < IE(M)). The "resolution" of the charge-transfer (CT) bracketing technique is limited by the IE difference of the neutrals used and is typically 0.1 eV. This technique was used by Eyler and co-workers[19] for the determination of the IEs of small ($n$

(11) Fürstenau, N.; Hillenkamp, F.; Nitsche, R. *Int. J. Mass Spectrom. Ion Phys.* **1979**, *31*, 85. Berkowitz, J.; Chupka, W. A. *J. Chem. Phys.* **1964**, *40*, 2735.

(12) O'Keefe, A.; Ross, M. M.; Baronavski, A. P. *Chem. Phys. Lett.* **1986**, *130*, 17.

(13) McElvany, S. W.; Creasy, W. R.; O'Keefe, A. *J. Chem. Phys.* **1986**, *85*, 632.

(14) McElvany, S. W.; Nelson, H. H.; Baronavski, A. P.; Watson, C. H.; Eyler, J. R. *Chem. Phys. Lett.* **1987**, *134*, 214.

(15) Creasy, W. R.; Brenna, J. T. *Chem. Phys.* **1988**, *126*, 453. So, H. Y.; Wilkins, C. L. *J. Phys. Chem.* **1989**, *93*, 1184. Lineman, D. N.; Somayajula, K. V.; Sharkey, A. G.; Hercules, D. M. *J. Phys. Chem.* **1989**, *93*, 5025. Campbell, E. E. B.; Ulmer, G.; Hasselberger, B.; Busmann, H. G.; Hertel, I. V. *J. Chem. Phys.* **1990**, *93*, 6900.

(16) McElvany, S. W.; Dunlap, B. I.; O'Keefe, A. *J. Chem. Phys.* **1987**, *86*, 715. Parent, D. C.; McElvany, S. W. *J. Am. Chem. Soc.* **1989**, *111*, 2393.

(17) McElvany, S. W. *J. Chem. Phys.* **1988**, *89*, 2063.

(18) Knight, R. D.; Walch, R. A.; Foster, S. C.; Miller, T. A.; Mullen, S. L.; Marshall, A. G. *Chem. Phys. Lett.* **1986**, *129*, 331.

(19) Bach, S. B. H.; Eyler, J. R. *J. Chem. Phys.* **1990**, *92*, 358.

164 *Acc. Chem. Res., Vol. 25, No. 3, 1992*

*McElvany et al.*
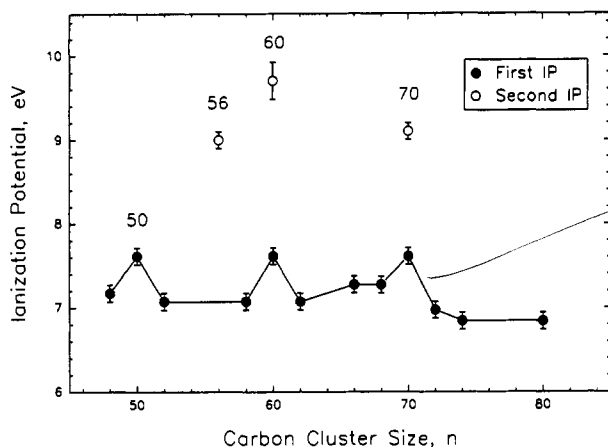


**Figure 2.** The first and second ionization energies of carbon clusters, $C_n$, determined by the charge-transfer bracketing technique.

< 24) carbon clusters. Large alternations were observed in the IEs, where the "magic-number" clusters ($n = 7$, 11, 15, etc.) have much lower IEs than their neighboring clusters, consistent with their enhanced abundances in the positive-ion mass spectrum.

The CT bracketing technique was subsequently used at the NRL to determine the IEs of the fullerenes.[20] These experiments were initiated prior to the production of bulk fullerenes; thus DLV of graphite was used to generate the corresponding fullerene cations in the FTMS. The results are shown in Figure 2 for selected $C_n$ with $48 \leq n \leq 80$. The neutral CT compounds used in this study included aromatic hydrocarbons, amines, and metallocenes. The IEs of the "magic-number" clusters ($n = 50, 60$, and 70) were determined to be 7.61 ± 0.11 eV. In contrast, the IEs of the neighboring fullerenes are considerably lower. Several aspects of these results were quite surprising. The alternations observed in the IEs resulting from the addition or subtraction of a $C_2$ unit are relatively large (~0.5 eV) for species of this size. Also, in contrast to the small carbon clusters ($n < 24$), the opposite trend is observed for the fullerenes in which the magic-number clusters in the positive-ion distribution possess relatively *high* IEs. This suggests that the enhanced abundance of these positive ions does not result from ease of ionization, but more probably from their greater absolute abundances as either neutrals or nascent ions. All of the carbon clusters (up to $n = 200$) were determined to have IEs significantly greater than the work function of graphite (4.9 eV), consistent with the recent structural confirmation of these species as a unique form of carbon. Although the $n = 50, 60$, and 70 clusters have the same IE, differences were observed in their reactivity with metallocenes. The reaction of $C_{60}^+$ and $C_{70}^+$ with metallocenes is significantly slower than that of the other clusters studied, including $C_{50}^+$. This reduced reactivity has been suggested to be consistent with closed-shell and/or extremely symmetrical structures. It is interesting that these species are also those produced and extracted in high abundance in the bulk synthesis of fullerenes.

The availability of macroscopic quantities of fullerenes has allowed the use of photoelectron[21] and pho-

toionization[22] spectroscopy for the determination of the IE of $C_{60}$. Photoelectron measurements in the bulk and gas phase yielded values of 7.6 ± 0.2 eV and 7.61 ± 0.02 eV, respectively. A value of 7.57 ± 0.01 eV has recently been reported using vacuum ultraviolet photoionization mass spectrometry.[22] The excellent agreement between these vertical IEs and the adiabatic value measured by CT indicates that little structural change occurs upon ionization, as would be expected from a relatively large, symmetrical molecule such as $C_{60}$.

Electron ionization of gas-phase fullerenes also results in the production of multiply-charged cations, which has allowed the bracketing of the second and third IEs of several fullerenes by the CT technique.[23] The second IEs are included in Figure 2 for $C_{60}$ (9.7 eV), $C_{70}$ (9.1 eV), and $C_{56}$ (9.0 eV). These second IEs are indicative of the stability of the singly-charged ion and are consistent with the observed mass spectrum, i.e., the enhanced stability (abundance) of $C_{60}^+$ and $C_{70}^+$. The second IEs of these large aromatic carbon clusters are low in comparison to those of similar systems, e.g., $p$-hexaphenyl ($C_{36}H_{26}$) has a first IE of 7.67 eV and a second IE of ~11.8 eV.[24] Considerably higher values have been estimated for the second IEs of $C_{60}$ by charge-stripping measurements (12.25 eV[25] and 11.9 eV[26]). Recent vacuum ultraviolet photoionization measurements[22] indicates a second IE intermediate to the charge-stripping and charge-transfer values, but the nonlinear behavior near threshold in the photoionization study favors the lower value.

The proton affinities (PA) of $C_{60}$ and $C_{70}$ have also been bracketed by ion/molecule reactions in the FTMS.[27] For these experiments, a mass-selected protonated reagent molecule ($MH^+$) is allowed to react with gas-phase fullerenes heated off a solids probe (reaction 2). Analogous to the CT bracketing method,

$$MH^+ + C_{60} (C_{70}) \rightarrow C_{60}H^+ (C_{70}H^+) + M \quad (2)$$

the occurrence (exothermicity) of reaction 2 indicates that $PA(C_n) > PA(M)$. The proton affinities of $C_{60}$ and $C_{70}$ were bracketed between ammonia and hexamethylbenzene, indicating that 204 kcal/mol ≤ PA-($C_{60}, C_{70}$) ≤ 207 kcal/mol. These values were confirmed by studying the proton-transfer reactions of $C_{60}H^+$ and $C_{70}H^+$ (i.e., the reverse of reaction 2). Also, proton transfer was observed from $C_{60}H^+$ to $C_{70}$, indicating that $PA(C_{70}) > PA(C_{60})$.

The stability of the protonated fullerenes was probed by CID.[27] These studies revealed that both protonated and unprotonated fullerenes are stable toward fragmentation in requiring relatively high-energy collisions ($E_{lab} > 150$ eV) with xenon. The protonated fullerenes dissociate at these energies solely by the loss of the hydrogen atom, in contrast to the underivatized fullerenes, which fragment by loss of one or more $C_2$ units. The H loss observed from $C_nH^+$ suggests that following

(20) Zimmerman, J. A.; Eyler, J. R.; Bach, S. B. H.; McElvany, S. W. *J. Chem. Phys.* **1991**, *94*, 3556.

(21) Lichtenberger, D. L.; Nebesny, K. W.; Ray, C. D.; Huffman, D. R.; Lamb, L. D. *Chem. Phys. Lett.* **1991**, *176*, 203.

(22) Yoo, R. K.; Ruscic, B.; Berkowitz, J. *J. Chem. Phys.*, in press.

(23) McElvany, S. W.; Ross, M. M.; Callahan, J. H. *Mater. Res. Soc. Symp. Proc.* **1991**, *206*, 697.

(24) Gallegos, E. J. *J. Phys. Chem.* **1967**, *71*, 1647.

(25) Lifshitz, C.; Iraqi, M.; Peres, T.; Fischer, J. *Rapid Commun. Mass Spectrom.* **1991**, *5*, 238.

(26) Caldwell, K. A.; Giblin, D. E.; Gross, M. L. *J. Am. Chem. Soc.*, in press.

(27) McElvany, S. W.; Callahan, J. H. *J. Phys. Chem.* **1991**, *95*, 6186.

proton transfer the charge is delocalized throughout the fullerene molecule.

High-pressure chemical ionization (CI) in a triple quadrupole mass spectrometer (TQMS) has been used as an alternative to electron ionization for the production of fullerene ions in several studies.[28] As expected, positive-ion CI results in the production of protonated fullerenes ($n$ = 60, 70, 76, 78, and 84) with no fragmentation. Negative-ion CI has been shown to be an extremely sensitive method for fullerene analysis because of the relatively high electron affinities of carbon clusters. In contrast to observations with positive-ion CI, fullerenes (even $n$) up to $n$ = 124 are observed as anions from thermal desorption of toluene extracts of soot using negative-ion CI.[27,28]

In addition to protonated fullerenes, many other fullerene derivatives have been generated by gas-phase ion/molecule reactions. The high-pressure CI conditions used to generate protonated fullerenes also result in adduct formation of the fullerenes with the reagent ions (e.g., $C_n \cdot C_2H_5^+$ with methane and $C_n \cdot C_4H_9^+$ with isobutane). These species undergo fragmentation to yield $C_nH^+$ at low energies ($E_{lab} \approx 50$ eV) and $C_n^+$ at higher energies, consistent with the relative proton affinities of the fragments and the $C_nH^+$ results discussed above. Negative-ion CI with oxygen has also been used to produce oxygen derivatives of buckminsterfullerene; products with up to six oxygen atoms can be formed ($C_{60}O_n^-$, $n$ = 1–6).[29] Low-energy CID studies show that $C_{60}O^-$ dissociates by loss of O, but that $C_{60}O_2^-$ and $C_{60}O_3^-$ fragment by loss of CO and $CO_2$. These results are consistent with other fullerene oxidation studies.[30]

## Fragmentation of Fullerenes

Smalley and co-workers reported the first systematic study of the fragmentation of $C_{60}^+$ in photodissociation/tandem TOF mass spectrometry experiments.[31] The primary fragmentation channel for $C_{60}^+$ is the loss of neutral $C_2$ units, and the activation energy for the initial $C_2$ loss was estimated to be 18 eV. With the availability of large quantities of fullerenes, it has been possible to conduct a wider range of MS/MS experiments. The low-energy collisional activation of $C_{60}^+$ was studied using both TQMS and a reverse-geometry hybrid mass spectrometer (BEQ).[32] When Xe is used as a collision gas (to increase the center-of-mass collision energy, $E_{cm}$, over that of He or Ar) under multiple-collision conditions (to improve energy transfer), $C_2$ loss is initially observed at collision energies of roughly 150
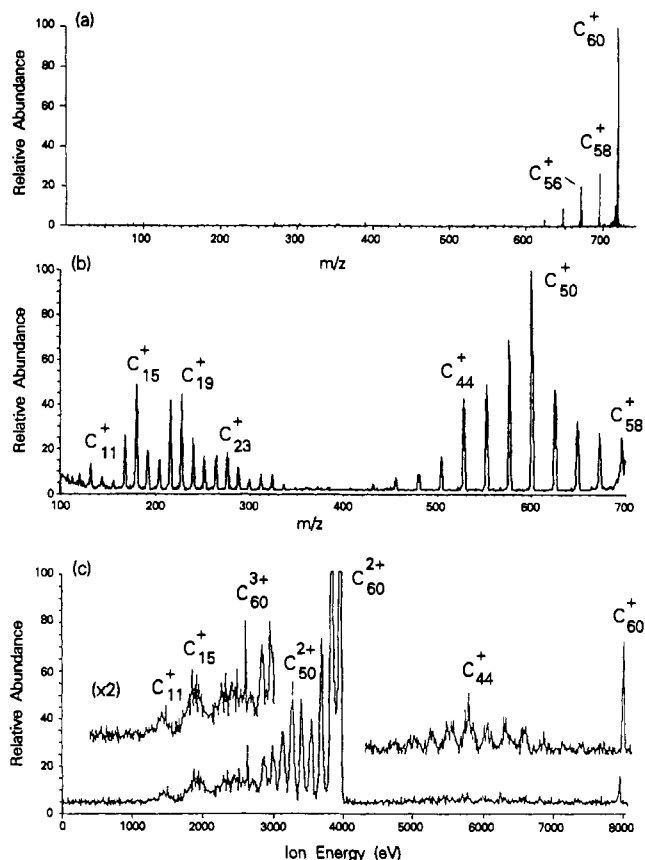


**Figure 3.** Collision-induced-dissociation spectra of (a) $C_{60}^+$ collisions with Xe at 190 eV in the TQMS (multiple-collision conditions); (b) $C_{60}^+$ collisions with Xe at 450 eV in the collision quadrupole of the BEQ instrument (multiple-collision conditions; the parent ion is not shown); (c) $C_{60}^{2+}$ collisions with He at 4 keV in the collision cell between B and E on the BEQ instrument (single collision, MIKE scans).

eV ($E_{cm} \sim 23$ eV).[27] Therefore, this energy represents the upper limit necessary to initiate $C_2$ loss, which is consistent with the photodissociation estimate.[31] Further increases in collision energy (e.g., 190 eV in Figure 3a) have the expected effect of inducing loss of additional $C_2$ units (or larger, even $C_n$ units) from the ion. Higher collision energies (450 eV, Figure 3b) result in fragmentation to give both high-mass products ($C_n^+$, even-number $n$ > 32) and low-mass products. The latter consist of both even- and odd-numbered carbon cluster ions. The spectrum shows that sequential $C_2$ loss ends in the region around $C_{34}^+$, consistent with the photodissociation results.[31] It should also be noted that the fragmentation products exhibit "magic-number" behavior in both the low- and high-mass $C_n^+$ distributions similar to those in the laser vaporization mass spectra (see Figure 1). The observation of these "magic numbers" in both production and fragmentation reflects the special stability of these clusters.

Several groups have investigated high-energy CID of the fullerenes.[33] Our studies have utilized mass-analyzed ion kinetic energy (MIKE) scans in which $C_{60}^+$ is selected by a magnetic sector (B) and fragmented by collisions with a target gas, and product ion kinetic energies are analyzed with an electric sector (E).[34] Only

(28) Cox, D. M.; Behal, S.; Disko, M.; Gorun, S.; Greany, M.; Hsu, C. S.; Kollin, E.; Millar, J.; Robins, J.; Robins, W.; Sherwood, R.; Tindall, P. *J. Am. Chem. Soc.* **1991**, *113*, 2940. Ben-Amotz, D.; Cooks, R. G.; Dejarme, L.; Gunderson, J. C.; Hoke, S. H.; Kahr, B.; Payne, G. L.; Wood, J. M. *Chem. Phys. Lett.* **1991**, *183*, 149.

(29) Callahan, J. H.; McElvany, S. W.; Doyle, R. J.; Ross, M. M. *Proceedings of the 39th ASMS Conference on Mass Spectrometry and Allied Topics*, Nashville, TN, May 19–24, 1991; p 420.

(30) Kroll, G. H.; Benning, P. J.; Chen, Y.; Ohno, T. R.; Weaver, J. H.; Chibante, L. P. F.; Smalley, R. E. *Chem. Phys. Lett.* **1991**, *181*, 112–116. Diederich, F. N.; Ettl, R.; Rubin, Y.; Whetten, R. L.; Beck, R.; Alvarez, M. M.; Anz, S.; Sensharma, D.; Wudl, F.; Khemani, K. C.; Koch, A. *Science* **1991**, *252*, 548.

(31) O'Brien, S. C.; Heath, J. R.; Curl, R. F.; Smalley, R. E. *J. Chem. Phys.* **1988**, *88*, 220.

(32) This instrument consists of a magnet (B), electrostatic analyzer (E), collision region, and analyzer quadrupole (Q); this instrument and its scan functions are described in the following: Harrison, A. G.; Mercer, R. S.; Reiner, E. J.; Young, A. B.; Boyd, R. K.; March, R. E.; Porter, C. J. *Int. J. Mass Spectrom. Ion Processes* **1986**, *74*, 13.

(33) Luffer, D. R.; Schram, K. H. *Rapid Commun. Mass Spectrom.* **1990**, *4*, 552. Young, A. B.; Cousins, L.; Harrison, A. G. *Rapid Commun. Mass Spectrom.* **1991**, *5*, 226.
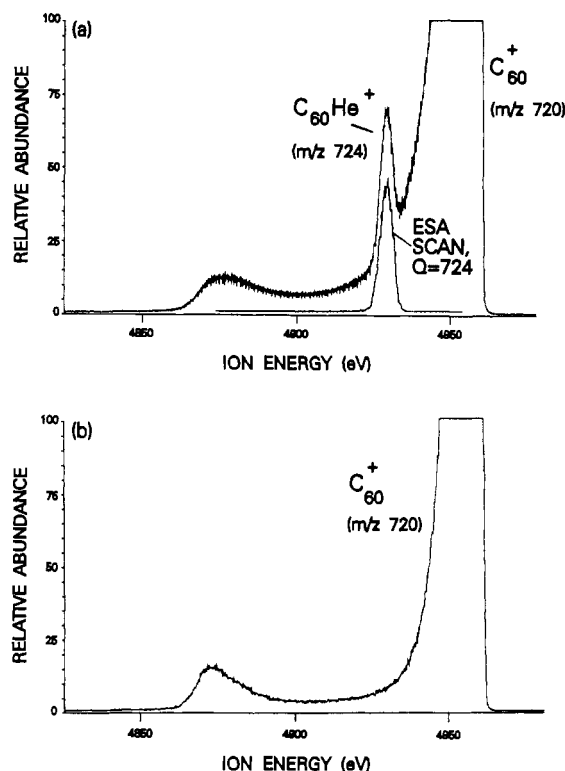
(34) Doyle, R. J.; Ross, M. M. *J. Phys. Chem.* **1991**, *95*, 4945.

a few high-mass products (e.g., $C_{48}^+$–$C_{58}^+$) are detected when He is used as a collision gas, because of the relatively small $E_{cm}$ (e.g., 44 eV in 8-keV collisions). However, use of heavier target gases ($O_2$, $N_2$) produces small carbon fragment ions with "magic numbers" similar to those in Figure 3b.[34] In addition, processes such as charge stripping (e.g., $C_{60}^+ \rightarrow C_{60}^{2+}$ in $O_2$ collisions) were observed and have been used by other groups to estimate the second ionization energy of $C_{60}$, as discussed earlier.[25,26] Similar results are obtained in the fragmentation of multiply-charged fullerenes.[34] For example, the high-energy fragmentation spectrum of $C_{60}^{2+}$ (Figure 3c) is characterized by both singly- and doubly-charged fragments, as well as charge reduction ($C_{60}^+$) and charge stripping ($C_{60}^{3+}$).

Inelastic ion/surface collisions have also been used to fragment $C_{60}^+$. This technique is referred to as surface-induced dissociation (SID) and has been developed by Cooks and co-workers.[35] SID is characterized by relatively efficient kinetic to internal energy transfer, with approximately 13% of $E_{lab}$ taken up as internal energy.[35,36] We have studied the surface collisions of $C_{60}^+$ with a stainless steel surface in two different tandem quadrupole instruments,[36] which are limited to collision energies of less than 130 eV. Under these conditions fragmentation of $C_{60}^+$ is not detected, consistent with the maximum estimated energy deposition of approximately 17 eV. However, fragmentation and charge reduction leading to $C_{58}^+$ and $C_{56}^+$ are observed in 130-V (260-eV) surface collisions of $C_{60}^{2+}$.[37] The estimated amount of energy deposited in this case (including that from charge reduction) is 43–46 eV; the absence of more extensive fragmentation in this case is puzzling. Whetten and co-workers[38] have studied collisions of $C_{60}^+$ with various surfaces in a reflectron TOF instrument and observed no detectable fragmentation at collision energies as high as 250 eV (~33-eV internal energy deposition at 13% conversion). This suggests that the kinetic to internal energy conversion in $C_{60}^+$ is not as efficient as expected. It has been speculated that the unique structure of $C_{60}$ results in a special resilience in the surface collision experiment.[38]

## Fullerene Endohedral Complexes: Formation by Gas-Phase Collisions

Another manifestation of the special structure of $C_{60}$ is observed in high-energy collisions of $C_{60}^+$ with small target gases. Schwarz and co-workers[39] noted that although $C_{60}^+$/He collisions yielded a few relatively high-mass products (e.g., $C_{48}^+$–$C_{58}^+$), the product ions appeared as multiple peaks. They used a four-sector instrument ($B_1E_1B_2E_2$) to obtain higher resolution product ion scans (in which $B_1E_1$ was used to select $C_{60}^+$ and a linked scan of $B_2E_2$ was used to analyze collision products). Their results showed that the region around each fragment consisted of the expected product ion

(35) Cooks, R. G.; Ast, T.; Mabud, Md. A. *Int. J. Mass Spectrom. Ion Processes* **1990**, *100*, 209.

(36) Wysocki, V. H.; Ding, J.-M.; Jones, J. L.; Callahan, J. H.; King, F. L. *J. Am. Soc. Mass Spectrom.* **1992**, *3*, 27.

(37) Callahan, J. H.; Ross, M. M.; Wysocki, V. H.; Jones, J. L.; Ding, J.-M. *Proceedings of the 39th ASMS Conference on Mass Spectrometry and Allied Topics*, Nashville, TN, May 19–24, 1991; p 829.

(38) Beck, R. D.; St. John, P.; Alvarez, M. M.; Diederich, F.; Whetten, R. L. *J. Phys. Chem.* **1991**, *95*, 8402. Beck, R. D.; Yeretzian, C.; St. John, P.; Whetten, R. L. *J. Phys. Chem.*, submitted.

(39) Weiske, T.; Böhme, D. K.; Hrušák, J.; Krätschmer, W.; Schwarz, H. *Angew. Chem., Int. Ed. Engl.* **1991**, *30*, 884.

**Figure 4.** The 5-keV $C_{60}^+$/He CID/MIKE spectrum showing ions that are transmitted through the electrostatic analyzer (a) over a narrow energy range that includes $C_{60}^+$ and (b) over the same energy range but with additional mass selection of $m/z$ 720 ions by the analyzer quadrupole. The peak identified as $[C_{60}He]^+$ in part was confirmed by setting the quadrupole to $m/z$ 724, as indicated by the overlapping scan marked ESA SCAN, Q = 724, in part a.

(e.g., $C_{58}^+$, $C_{56}^+$) and an additional peak 4 mass units higher (e.g., $C_{58}^+ + 4$, $C_{56}^+ + 4$). When the collision gas was changed to $^3$He, the difference between the peaks decreased to 3 mass units. The conclusion drawn from this unprecedented result was that $C_{60}^+$ takes up He in the collision and subsequently fragments to yield $C_nHe^+$ products. Schwarz and co-workers initially did not report observation of the $[C_{60}He]^+$ complex, but noted similar results in collisions with Ne.

Schwarz's initial difficulty in detecting the $[C_{60}He]^+$ product was the result of the energetics of the collision process. If He is taken up by the collision partner in a perfectly inelastic collision, all of $E_{cm}$ is taken up as internal energy (e.g., 44 eV in an 8-keV collision), and the $[C_{60}He]^+$ product has a reduced kinetic energy (by 44 eV). Thus, the product has a lower kinetic energy but higher mass than the original projectile, making it difficult to observe $[C_{60}He]^+$ in certain product ion scans. However, using the hybrid instrument (BEQ), we were able to show unambiguously that a $[C_{60}He]^+$ product was formed.[40,41] Figure 4a shows the MIKE scan around the parent-ion region for 5-keV collisions of $C_{60}^+$ with He (single-collision conditions). The spectrum is characterized by a distinct peak at 4925 eV which appears as a shoulder on the transmitted $C_{60}^+$ beam (off-scale). Figure 4b shows the scan obtained when the magnet (B) is used to select $C_{60}^+$, the analyzer quadrupole (Q) is set to pass $m/z$ 720 ($C_{60}^+$), and the

(40) Ross, M. M.; Callahan, J. H. *J. Phys. Chem.* **1991**, *95*, 5720.

(41) Mowrey, R. C.; Ross, M. M.; Callahan, J. H. *J. Phys. Chem.*, submitted.

electric sector (E) is scanned (MIKE scan with fixed Q). This scan shows the kinetic energy spectrum of the $C_{60}^+$ ions only, which clearly does not include the feature of 4925 eV in Figure 4a. However, superimposed on Figure 4a is the MIKE scan obtained when the quadrupole is set to pass $m/z$ 724 ($[C_{60}He]^+$). This scan confirms that the feature at 4925 eV arises from $[C_{60}He]^+$, which appears at a kinetic energy shifted lower from that of the $C_{60}^+$ beam by 26 eV; this is consistent with an $E_{cm}$ of 27.3 eV at 5 keV. Similar analyses for the $C_n^+$ fragment regions confirmed Schwarz's observation of $[C_nHe]^+$ fragments.

Experiments utilizing other capabilities of the hybrid instrument have given further insight into the nature of the $C_{60}^+$/He product. Selecting $C_{60}^+$ with the magnet and setting the electric sector voltage for the maximum transmission of $[C_{60}He]^+$ allows these ions (and some overlapping $C_{60}^+$) to be transmitted into the quadrupoles. Scanning the analyzer quadrupole yields a mass spectrum that includes both $C_{60}^+$ and $[C_{60}He]^+$, as well as some $[C_{58}He]^+$ formed by unimolecular decomposition of the internally excited $[C_{60}He]^+$ complex. When Xe is admitted to the collision quadrupole and $[C_{60}He]^+$ undergoes 200-eV collisions, $[C_{54}He]^+$ and $[C_{56}He]^+$ fragments are observed in addition to $[C_{58}He]^+$ and $[C_{60}He]^+$. Under these multiple-collision conditions, it is unlikely that $[C_{60}He]^+$ would survive if He were bound to the exterior of $C_{60}^+$ by van der Waals or ion-induced-dipole interactions. These results strongly suggest that He is in the interior of $C_{60}^+$, indicating an endohedral complex ($(He@C_{60})^+$ using the Smalley nomenclature[42]), as Schwarz hypothesized.

The production of endohedral fullerene complexes by gas-phase collisions continues to be an active area of research in several laboratories.[26,43,44] Schwarz and co-workers have shown that similar phenomena occur with multiply-charged fullerenes.[44] Gross and co-workers have observed adducts of $C_n^+$ with $D_2$, Ar, and Ne[43] and have shown that two He atoms can be taken up by $C_{70}^+$ when it undergoes multiple collisions with He.[26] They also provided evidence for an inelastic scattering tail in the $C_{60}^+$ kinetic energy spectrum. Both groups have demonstrated that the intact $C_{60}He^+$ fragment can be detected with a four-sector mass spectrometer.[26,43,44] Two other groups have recently reported measurements of the energetics of this process.[45]

In order to obtain further insight into the formation of endohedral complexes in high-energy collisions, we are collaborating with the theoretical chemistry group at the NRL to model the He/$C_{60}$ collision process by molecular dynamics simulations.[41,46] The simulations predict that a maximum trapping efficiency of 15% should occur with 8-keV collisions, while the experiment
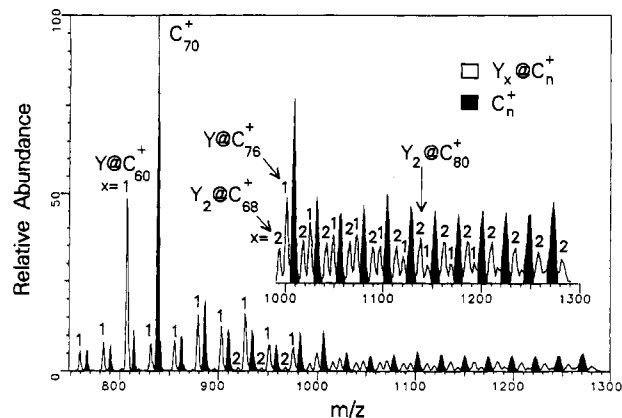


**Figure 5.** Mass spectrum resulting from direct laser vaporization of a sample containing a mixture of graphite, yttrium oxide ($Y_2O_3$), and bulk fullerenes. In addition to the production of carbon cluster cations, $C_n^+$, yttrium-containing fullerenes ($(Y@C_n)^+$ and $(Y_2@C_n)^+$) are also observed.

shows that a maximum trapping efficiency of 6% is observed in 5-keV collisions. The difference between theory and experiment can be explained mainly by the unimolecular decomposition of internally excited $(He@C_{60})^+$, since all of $E_{cm}$ is converted to internal energy in the complex. The rate of unimolecular decomposition will increase with increasing collision energy, resulting in lower abundances than predicted, particularly at higher energy. The simulations also suggest that the inelastic scattering "foot" observed in $C_{60}^+$/He collision spectra (see Figure 4b) can be explained in terms of an impulsive collision and momentum transfer between He and, effectively, one or two carbon atoms in $C_{60}^+$.

## Fullerene Endohedral Complexes: Formation by Laser Vaporization

The potential unique properties of endohedral metallofullerenes have been postulated since the initial reports on the production of these species in the gas phase.[5,47] The recent synthesis of macroscopic quantities of these materials will facilitate their complete characterization.[42,48] We have recently been interested in generating these species by DLV and characterizing their gas-phase properties. Direct laser vaporization (i.e., no molecular beam expansion) of mixed graphite/yttrium oxide ($Y_2O_3$) samples (~9:1 wt %) produces abundant $Y^+$ and $YO^+$ but no carbon cluster ions, presumably due to the relatively low IEs of Y and YO (6.2 and 5.85 eV, respectively). Similar samples have been used with molecular beam sources to generate endohedral $(M@C_n)^+$, where M is an alkali metal[47] or an early transition metal (e.g., lanthanum[5,42]). However, $YC_n^+$ species are generated by DLV if the sample is "seeded" with a small amount of bulk fullerenes ($C_{60}$ and $C_{70}$). Figure 5 shows the positive-ion mass spectrum resulting from DLV of a graphite/$Y_2O_3$/fullerene mixture (~7:2:1 wt %). In addition to the presence of fullerene cations ($C_{64}$–$C_{106}^+$), there are peaks corresponding to $YC_n^+$ ($n$ = 56–96) with an enhanced abundance of $YC_{60}^+$ ($m/z$ 809). At higher $m/z$, additional peaks are observed which correspond to $Y_2C_n^+$

(42) Chai, Y.; Guo, T.; Jin, C.; Haufler, R. E.; Chibante, L. P. F.; Fure, J.; Wang, L.; Alford, J. M.; Smalley, R. E. *J. Phys. Chem.* **1991**, *95*, 7564.

(43) Caldwell, K. A.; Giblin, D. E.; Hsu, C. S.; Cox, D.; Gross, M. L. *J. Am. Chem. Soc.* **1991**, *113*, 8519.

(44) Weiske, T.; Hrusak, J.; Bohme, D. K.; Schwarz, H. *J. Phys. Chem.* **1991**, *95*, 8451. Weiske, T.; Hrusak, J.; Bohme, D. K.; Schwarz, H. *Chem. Phys. Lett.* **1991**, *186*, 459. Weiske, T.; Hrusak, J.; Bohme, D. K.; Schwarz, H. *Helv. Chim. Acta*, in press.

(45) Wan, Z.; Christian, J. F.; Anderson, S. A. *J. Phys. Chem.*, submitted. Campbell, E. E. B.; Ehlich, R.; Hielscher, A.; Frazao, J. M. A.; Hall, I. V. *Z. Phys. D*, in press.

(46) For details of the simulations, see: Mowrey, R. C.; Brenner, D. W.; Dunlap, B. I.; Mintmire, J. W.; White, C. T. *J. Phys. Chem.* **1991**, *95*, 7138.

(47) Weiss, F. D.; Elkind, J. L.; O'Brien, S. C.; Curl, R. F.; Smalley, R. E. *J. Am. Chem. Soc.* **1988**, *110*, 4464.

(48) Alvarez, M. M.; Gillan, E. G.; Holczer, K.; Kaner, R. B.; Min, K. S.; Whetten, R. L. *J. Phys. Chem.* **1991**, *95*, 10561. Johnson, R. D.; de Vries, M. S.; Salem, J.; Bethune, D. S.; Yannoni, C. S. *Nature*, submitted.

and are maximum for $n = 68$–$90$. The $Y_2C_n^+$ species become more abundant than the corresponding $YC_n^+$ species for $n > 82$.

The origin and structure of the $Y_xC_n^+$ species generated by DLV are unclear. The presence of bulk fullerenes in the sample may be expected to result in gas-phase recombination of $Y^{+/0}$ and $C_n^{0/+}$ to produce an externally-bound species, e.g., $Y(C_{60})^+$. However, the dependence of the $Y_xC_n^+$ signal on laser conditions (irradiation time and fluence) indicates that these species may form in the bulk through coalescence reactions, as has recently been postulated for $La_2O_3/$ graphite samples in a molecular-beam source.[42] This would suggest that the $Y_xC_n^+$ species have endohedral structures. This surprising result was confirmed by their oxidative stability in reactions with $N_2O$. The $Y_xC_n^+$ in Figure 5 are unreactive with $N_2O$,

$$Y_xC_n^+ + N_2O \rightarrow \text{no reaction}$$
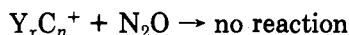
consistent with the metal atom(s) residing within the carbon cage, because the bare metal ion, $Y^+$, oxidizes readily under similar conditions to form $YO^+$. In addition, the isomeric externally-bound $Y(C_{60})^+$ species generated by the gas-phase association reaction

$$Y^+ + C_{60} \rightarrow Y(C_{60})^+ \xrightarrow{+N_2O} YO^+ + [C_{60} + N_2]$$
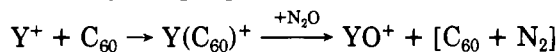
is also unstable toward oxidation, providing conclusive evidence that the DLV-generated species are endohedral complexes, $(Y_x@C_n)^+$. We are currently characterizing these gas-phase species by their ion/molecule reactions (e.g., IE determination by CT bracketing) in addition to attempting to obtain a better understanding of their formation mechanism.

## Summary and Prospective

Mass spectrometric studies of the fundamental aspects of the production and properties of gas-phase carbon clusters led to the discovery of a new form of carbon. In particular, the early experiments yielded insights into the cluster formation process and cluster properties, such as stability and reactivity, which provided evidence for the proposed fullerene cage structures. The availability of macroscopic quantities of fullerenes has allowed further mass spectrometry experiments, with different ionization and dissociation techniques, revealing some physical and chemical properties.

Several mass spectrometric methods are being employed to characterize fullerene derivatives. A major challenge for mass spectrometrists is to develop improved techniques for analysis of high-mass, intractable species, such as fullerene-based polymers and pure or derivatized "giant" fullerenes. The recent development of ionization techniques such as matrix-assisted laser desorption and electrospray, which have produced ions from molecules with molecular weights in excess of $100\,000$ amu, may be useful in addressing these challenges. Fullerenes derivatized with encapsulated species, endohedral complexes, represent a unique opportunity, and initial work has shown that mass spectrometry is important in both their synthesis and characterization. As work proceeds on large-scale production and isolation of internally-doped fullerenes, research on the gas-phase chemistry of these novel species will guide condensed-phase, synthetic chemistry. As with the pure (undoped) fullerenes, mass spectrometry studies of the fullerene endohedral complexes will likely lead to another unique class of materials.